JOURNAL OF GEOPHYSICAL RESEARCH, VOL. 106, NO. B3, PAGES 4207–4219, MARCH 10, 2001

Prehistoric fault offsets of the Hilina fault system, south flank of Kilauea Volcano, Hawaii

Eric C. Cannon[1]

Department of Geology, University of California, Davis, California

Roland Bürgmann

Department of Geology and Geophysics, University of California, Berkeley, Berkeley, California

Abstract. Historical accounts of earthquakes on the Island of Hawaii date only to 1823 but lava flows as old as 1500-3000 years B.P. contain fault offsets from prehistoric earthquakes. The *M*7.2 1975 Kalapana earthquake produced over 25 km of fault rupture along the Hilina fault system. We compare fault offsets in prehistoric lava flows with Kalapana earthquake fault offsets in neighboring 1969-1974 Mauna Ulu lava flows to estimate the frequency of prehistoric major earthquakes on the Hilina fault system. Horizontal and vertical fault offset rates across the Hilina fault system are 4.0 to 12.0 and -2.0 to -20.0 mm/yr, respectively, based on lava flows <750 years B.P. age. Assuming prehistoric earthquakes produced similar fault offsets compared to the Kalapana earthquake, three to five events are recorded in 400-750 years B.P. old lava flows yielding recurrence intervals of 260-80 years. Vertical fault offsets in prehistoric lava flows suggest that hanging wall rotation of the Hilina fault system contributes to fault offset. The assumption that past faulting resulted from prehistoric earthquakes with similar magnitude and fault offset to the Kalapana earthquake is an oversimplification. Large south flank earthquakes most likely do not have uniform recurrence intervals.

1. Introduction

The south flank of Kilauea Volcano, Hawaii has experienced two large (*M*>7) earthquakes in historic times, the 1975 *M*7.2 Kalapana and 1868 *M*7.9 Great Kau earthquakes (Figure 1) [*Ando*, 1979; *Furumoto and Kovach*, 1979; *Tilling et al.*, 1975; *Lipman et al.*, 1985; *Wyss*, 1988]. The average recurrence interval of large prehistoric earthquakes, however, remains disputed [*Wyss and Koyanagi*, 1992]. Catastrophic landslides and submarine slumps triggered by large south flank earthquakes pose a significant hazard to the Hawaiian Islands [*Lipman et al.*, 1985; *Moore et al.*, 1995; *Ma et al.*, 1999]. Local tsunamis produced by the 1975 Kalapana and 1868 Great Kau earthquakes reached maximum heights of ~15 m and ~14 m respectively. On a regional scale, tsunamis generated by future catastrophic south flank failures may threaten cities in the Pacific region.

This research evaluates past motions on the Hilina fault system associated with large south flank earthquakes. Records of historical seismicity on the Island of Hawaii only extend back to 1823 [*Wyss and Koyanagi*, 1992]. Thus estimates of pre-1823 fault offset require field measurements of surface rupture caused by large earthquakes. Triggered slip along the normal faults of the Hilina fault system recorded in prehistoric lava flows is the only accessible source of geologic information about prehistoric earthquakes. We first document ground fractures from the 1975 Kalapana earthquake (hereinafter referred to as the Kalapana earthquake). The Kalapana earthquake is the only large south flank earthquake documented with geodetic measurements of displacement, seismicity, and fault offset measurements along the Hilina fault system. We then compare the Hilina fault offsets from the Kalapana earthquake and the fault offsets in prehistoric dated lava flows to estimate the number of similar earthquakes to have struck the south flank in the past ~1500-3000 years. Our characterization of the past faulting behavior of the Hilina fault system provides new constraints for future earthquake, landslide, and tsunami hazard assessments of the south flank.

2. South Flank Tectonic Setting

Seismicity, geologic structures, and geodetic observations of deformation define the geometry and movement of the south flank block. The wedge-shaped mobile south flank block is bounded at ~8-10 km depth by a shallowly landward dipping basal detachment fault. The basal detachment fault is illuminated by microseismicity beneath the upper south flank [*Ando*, 1979; *Got et al.*, 1994; *Gillard et al.*, 1996] and imaged offshore at shallower depths in seismic reflection data [*Morgan et al.*, 2000]. The basal detachment fault may develop along a weak boundary layer composed of ocean sediments deposited on the Cretaceous ocean floor [*Hill*, 1969; *Nakamura*, 1980; *Thurber and Gripp*, 1988]. Focal mechanism studies of the Kalapana earthquake main shock and its aftershock sequence indicate southeast transport of the

[1]Now at Department of Geological Sciences, University of Colorado, Boulder, Colorado.

Paper number 2000JB900412.
0148-0227/01/2000JB900412$09.00

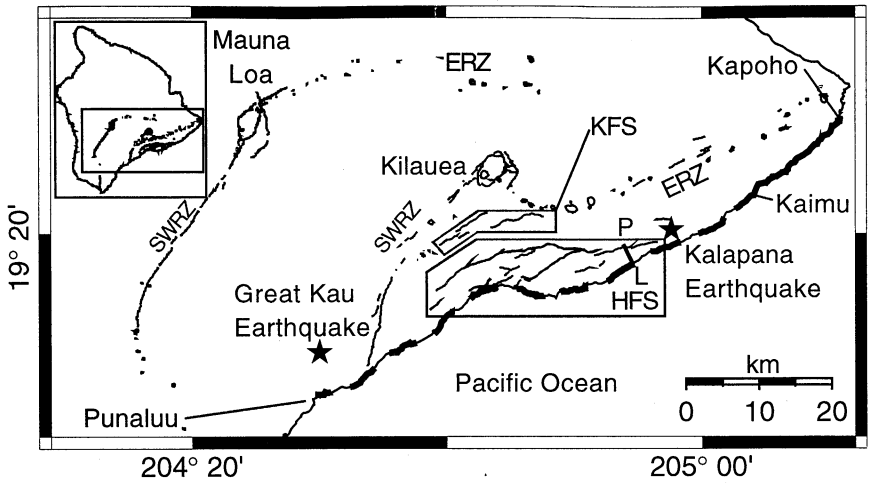

Figure 1. Location map for south flank of Kilauea Volcano, Hawaii. Stars locate epicenters for 1975 Kalapana and 1868 Great Kau earthquakes. Heavy dashed line indicates region of coastal subsidence for Kalapana earthquake from Punaluu to Kaimu; coastal subsidence from Great Kau earthquake probably extended farther northeast (heavier bold line) to Kapoho [*Wyss*, 1988]. Abbreviations represent KFS, Koae fault system; HFS, Hilina fault system; ERZ, east rift zone; SWRZ, southwest rift zone. Rupture of Hilina fault system in Kalapana earthquake is shown with bold lines [*Lipman et al.*, 1985]. P-L represents Panau-Laeapuki geodetic baseline. Inset shows location of map on island.

south flank along the basal detachment fault [*Ando*, 1979; *Furumoto and Kovach*, 1979; *Gillard et al.*, 1996].

The Hilina fault system indicates collapse of the south flank block along the southern coastline of Hawaii (Figure 2). Up to 500 m of vertical offset occurs along the Hilina morphological scarps. The fault geometry is interpreted as either faults splaying off the basal detachment [*Lipman et al.*, 1985] or as shallow normal faults [*Swanson et al.*, 1974; *Ando*, 1979; *Hill and Zucca*, 1987; *Gillard et al.*, 1996]. A steeply southeast dipping lateral gradient in *P* wave velocity extending down to 10 km depth suggests that the Hilina faults descend to the basal detachment [*Okubo et al.*, 1997]. Alternatively, models of landward rotated lava flows assuming slip on a cylindrical fault surface suggest that the Puu Kapukapu fault descends to only 5.2 km *depth [Riley et al.*, 1999]. Fault offset measurements and geodetic data from the Kalapana earthquake suggest that the Hilina faults are a set of shallow normal faults (E. C. Cannon et al., Normal faulting and block rotation associated with the Kalapana earthquake, Kilauea Volcano, Hawaii, submitted to *Bulletin of the Seismological Society of America*, 2000). *Morgan et al.* [2000] interpreted several seismic reflectors offshore of the south flank as a possible 2-3 km deep detachment linked to the Hilina fault system.

A combination of rift zone dike intrusions [*Fiske and Jackson*, 1972; *Swanson et al.*, 1974; *Denlinger and Okubo*, 1995] and gravitational spreading [*Dieterich*, 1988; *Delaney et al.*, 1998] produce coseismic and asesicmic motion of the south flank to the southeast. A variety of geodetic studies, including triangulation, trilateration, leveling, and Global Positioning System (GPS) measurements, have detected overall seaward motion of the south flank since 1896 [*Swanson et al.*, 1974; *Lipman et al.*, 1985; *Owen et al.*, 1995; *Delaney et al.*, 1998]. Geodetic station Panau ("P" in Figure 1) has moved seaward at least 10 m horizontally since 1896, with ~4 m of horizontal displacement from the Kalapana earthquake and the remaining amount by aseismic slip along the basal detachment [*Swanson et al.*, 1974]. Between 1990 and 1996, GPS stations indicated south flank horizontal displacement rates of up to 10 cm/yr [*Owen et al.*, 1995, 2000]. Models of observed displacement rates require 15-25 cm/yr slip on a 9-km-deep horizontal detachment [*Owen et*

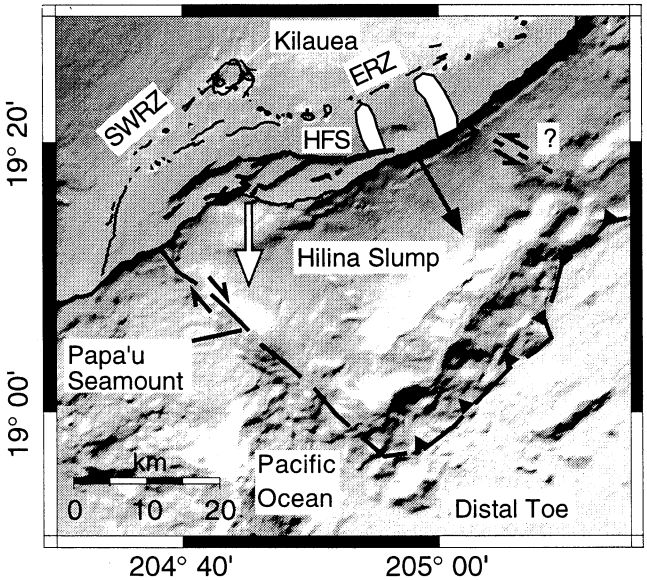

Figure 2. Shaded relief map of topography and bathymetry for south flank (digital topographic and bathymetric data provided by J. Smith [*Chadwick et al.*, 1993]). Artificial illumination from the northwest. Heavy black lines indicate trace of Hilina fault system (HFS). East rift zone (ERZ) and southwest rift zone (SWRZ) are identified. Two outlined white regions indicate areas of low electrical resistivity [*Flanigan and Long*, 1987]. Open arrow indicates motion of Hilina slump toward western boundary; solid arrow indicates more southeast directed motion of south flank; long-dashed solid line represents western boundary of Hilina (from *Morgan et al.* [2000]). Solid dashed lines with triangles indicate distal extent of hanging wall for south flank; short-dashed solid line may represent eastern boundary.

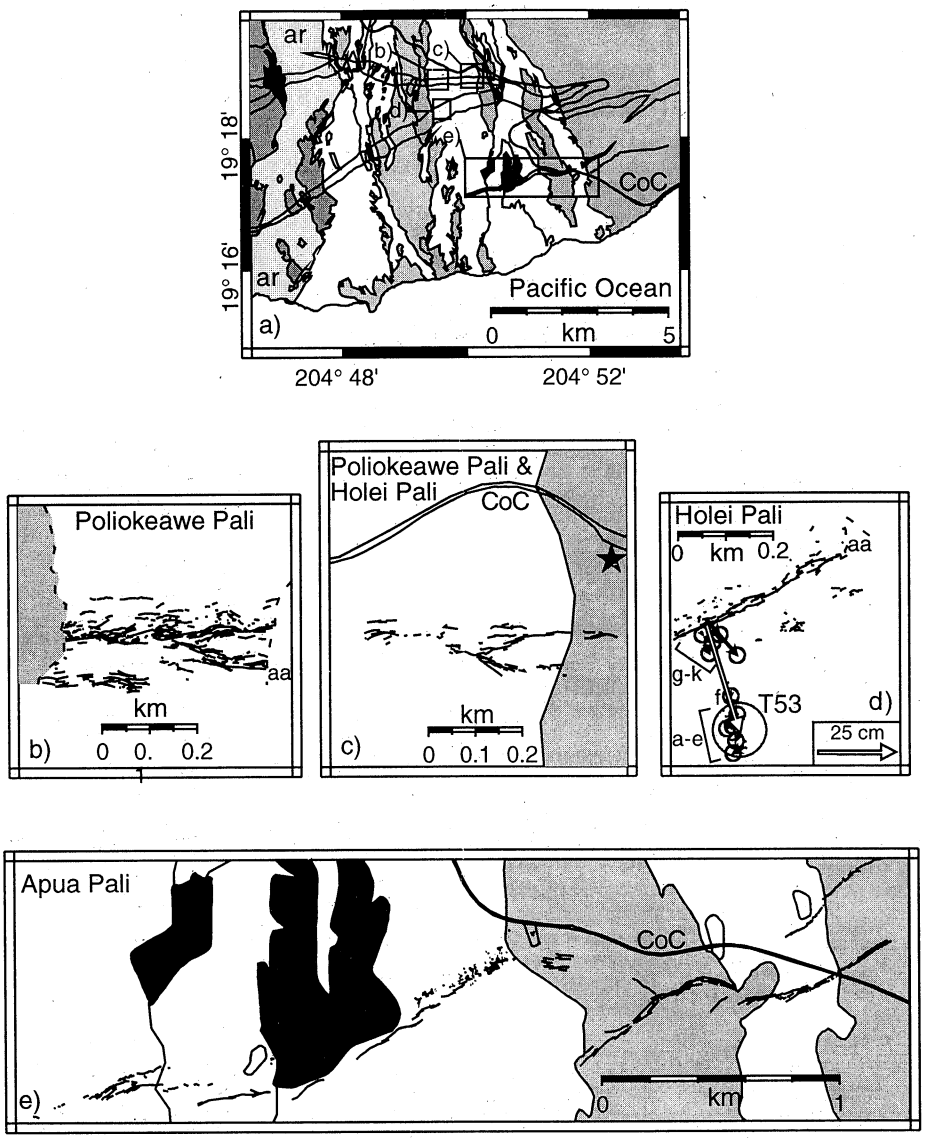

Figure 3. Location map for 1975 Kalapana earthquake ground fractures. (a) Lava flows of central Hilina fault system, ages defined in Figure 4. Chain of Craters Road labeled (CoC). Lettered boxes in Figure 3a show locations of Kalapana earthquake fractures on the (b) Poliokeawe Pali, (c) Poliokeawe & Holei Pali, (d) Holei Pali, and (e) Apua Pali faults. Figure 3d is an example of method to calculate fault offset traverses across a fault scarp: horizontal fault offset vector T53 (open vector) is sum of individual horizontal fault offset measurements "a" through "g" (solid vectors). Scale vector for both solid and open vectors is 25 cm.

al., 1995]. Whereas geodetic baselines across the south flank show significant extension and contraction since the Kalapana earthquake, baselines changes across the Hilina fault system suggest that the Hilina faults have not significantly displaced since the Kalapana earthquake [*Delaney et al.*, 1998].

3. The Kalapana and Great Kau Earthquakes

The *M*7.2 Kalapana earthquake is the largest earthquake to strike the south flank in the twentieth century [*Tilling et al.*, 1976]. An estimated 1000 km^2 of fault surface area ruptured on the basal detachment [*Lipman et al.*, 1985]. Coastal geodetic stations moved up to 8 m horizontally and subsided as much as 3.5 m [*Tilling et al.*, 1976; *Lipman et al.*, 1985]. Approximately 60 km of coastline from Punaluu to Kaimu (Figure 1) subsided due to the Kalapana earthquake [*Lipman et al.*, 1985]. Over 25 km of surface rupture occurred along the Hilina faults with a maximum of 1.5 m vertical offset (Figure 1) [*Tilling et al.*, 1976].

The 1868 *M*7.9 Great Kau earthquake (hereinafter referred to as the Great Kau earthquake) is the largest historical earthquake to occur in Hawaii (Figure 1). The earthquake sequence included a *M*~6.7 foreshock on March 28, 1868, the *M*7.9 main shock on April 2, 1868, and possibly a decade of aftershock activity [*Wyss*, 1988]. A ~14-m-high tsunami inundated coastal villages along the south flank coast [*Tilling et al.*, 1976; *Wyss*, 1988; *Wyss and Koyanagi*, 1992]. *Brigham* [1909] reported 1.2–2.1 m of permanent coastal subsidence along ~80 km of coastline from Punaluu to Kapoho (Figure 1). *Wyss* [1988] estimated 8 m of horizontal slip over a basal detachment area of 4000 km^2 bounded by Mauna Loa's rift zones.

4. Methods of Determining Fault Offsets and Time-Averaged Offset Rates

To improve our understanding of faulting behavior of the Hilina fault system prior to the Kalapana earthquake, we measure Hilina fault offsets of historic and prehistoric lava flows. Using piercing points, we measure fault offsets to determine plunge, azimuth, and total length of offset for faults. We utilize Global Positioning System Real-Time Kinematic (GPS-RTK) equipment and measuring tape and compass techniques to measure offsets. While compiling a fracture map of the Kalapana earthquake breaks, we obtained piercing point measurements with the GPS-RTK equipment with 1-2 cm horizontal and 2-4 cm vertical accuracy. In rugged terrain or more remote field locations where GPS-RTK equipment was impractical, we used the measuring tape and compass technique. We estimate our horizontal and vertical measurement error in obtaining a piercing point attitude with the measuring tape and compass technique to be ±1 cm.

Fault offset measurements across a fault zone are collected in traverses conducted perpendicular to the main fault traces of the Hilina faults (Figure 3d). Fault offset does not occur on one major fault strand but rather across a zone of distributed fractures. For each traverse, individual fault offsets are summed to calculate total fault offset for the traverse. For example, individual horizontal measurements of fault offset "a" through "k" (11 measurements) are summed to produce horizontal fault offset T53 (Figure 3). Vertical measurements for a traverse are calculated using the same method. Table 1 contains fault offsets for 85 traverses conducted across the Hilina fault system based on over 700 individual fault offset measurements. Error bounds for fault offset traverses containing multiple piercing point offsets equal the $\sqrt{(\sum}$ of the (measurement errors)^2).

Time-averaged calculations for fault offset rates require fault offset measurements recorded in dated lava flows (Figure 4). We use ages for south flank lava flows defined in "years before present relative to 1950" (years B.P). *Wolfe and Morris* [1996] utilized several methods to date lava flows including observed stratigraphic relationships, alteration of lava flow surfaces from an initially glassy surface, radiocarbon ages from charcoal samples [*Lockwood and Lipman*, 1980], and paleomagnetic secular variation [*Holcomb*, 1987]. Ages of south flank lava flows are assigned to five intervals: 1969-1974 Mauna Ulu, 200-750 years B.P., 400-750 years B.P., 750-1500 years B.P., and 1500-3000 years B.P. [*Wolfe and Morris*, 1996]. Two lava flows have ages of 350-450 and 2350-2450 years B.P. determined using radiocarbon dating methods (D. A. Swanson, personal communication, 2000). Given a lava flow of known age, a minimum time-averaged fault offset rate is calculated by dividing the fault offset for a given traverse by known age of the lava flow containing the traverse. This time-averaged calculation is a theoretical minimum fault offset rate because faulting probably occurred sometime after the lava flow cooled. We discuss the implications of the wide ranges of lava flow ages and minimum fault offset rates in section 7.

5. Kalapana Earthquake Ground Fracture and Fault Offset Data

The first step in understanding past faulting behavior of the Hilina fault system requires study of the ground fracture and fault offsets of the Kalapana earthquake. We present the first ground fracture map for the Kalapana earthquake (Figure 3b-3e). Mauna Ulu lava flows from 1969-1974 cover the central south flank region in pahoehoe and aa lava flows. These flows were fractured along the Hilina faults during the Kalapana earthquake (*Cannon et al.*, submitted manuscript, 2000). Single fractures extend as far as 170 m in length and fracture zones span a width of up to 200 m (Figure 3b). Fault ramps and steps produce fractures distributed throughout the fracture zone, not necessarily concentrated at the northern or southern boundaries of the fracture zone (Figures 3b-3e).

To determine fault offset of the Hilina fault system associated with the Kalapana earthquake, we present fault traverses in Mauna Ulu lava flows (solid vectors in Figure 5). Maximum horizontal and vertical fault offsets occur on the Holei Pali fault, with 2.8 m of horizontal offset and 1.6 m of vertical offset determined from a fault traverse containing 16 individual piercing point measurements. For each traverse we define the plunge of the slip vector as the arctangent of vertical fault offset divided by horizontal fault offset (Table 2). The average plunge of slip vectors for traverses across the Poliokeawe Pali, Holei Pali, and Apua Pali faults are 23°±24°, 23°±07, and 13°±15° respectively. For all plunges of slip vectors for the Hilina fault system the average plunge is 20°±17°.

6. Fault Offsets in Prehistoric Lava Flows

We measure the Hilina fault offsets in prehistoric lava flows (open vectors in Figure 5) to extend our knowledge about south flank earthquakes as far back as 1500-3000 years B.P. We are interested in determining fault offsets and fault offset rate for individual faults and across the Hilina fault system. The quality of fault offset preservation decreases with increased flow age. Lava flows less than 750 years B.P. age preserve sawtooth-shaped fractures and produce piercing points that can be easily measured. Lava flows with ages greater than 750 years B.P. have degraded fracture surfaces that make fault offset measurements difficult or impossible to obtain. Often with flows older than 750 years B.P., only estimates of scarp height are obtained with error estimates of a few meters. When a piercing point is not preserved, no measurement of horizontal or vertical fault offset can be determined.

To estimate the number of large earthquakes that have occurred on Hilina faults, we collect offset data at locations with two important requirements. First, prehistoric lava flows and Mauna Ulu flows must be juxtaposed. Second, fault offsets in prehistoric lava flows must be well-preserved so piercing points can be measured. The Kealakomo Overlook region meets both of these requirements (Figure 6). The Mauna Ulu lava flows are bounded to the east and west by 400-750 years B.P. age lava flows. Traverses span both the Poliokeawe Pali and Holei Pali with traverses A and D located in the prehistoric lava flows and traverses B and C located in the Mauna Ulu lava flows. Fault offsets in the Mauna Ulu lava flows display 1-2 m horizontal offset and 0.2-0.5 m vertical offset. Fault offsets in the prehistoric lava flows show 2-3 m horizontal fault offset and 3-4 m vertical fault offset.

Analyzing fault offsets relationships at double-fracture outcrop locations is another method used to estimate the recurrence interval of large earthquakes. We define a double-fracture outcrop in four stages using the following example.

Table 1. Fault Offsets Calculated Along Traverses[a]

			Offset, m			Error Bound, m		
Traverse	Longitude	Latitude	East	North	Vertical	East	North	Vertical
1	-155.20572	19.32192	0.108	-8.760	-0.258	0.022	0.022	0.022
2	-155.20889	19.32164	0.031	-0.108	-0.060	0.010	0.010	0.010
3	-155.20485	19.31841	0.048	-1.154	-5.248	0.041	0.041	0.041
4	-155.20294	19.31936	1.210	-1.392	-1.340	0.041	0.041	0.041
5	-155.20261	19.32130	1.148	-1.523	-0.379	0.143	0.143	0.143
6	-155.20306	19.32126	-0.022	0.014	-0.114	-0.318	0.014	0.014
7	-155.20297	19.32126	0.034	-0.964	-0.223	0.010	0.010	0.010
8	-155.19817	19.32029	-0.132	-0.763	-2.501	0.030	0.030	0.030
9	-155.19283	19.32075	0.118	-1.868	-0.528	0.044	0.044	0.044
10	-155.20053	19.29205	0.403	-1.492	-0.217	0.110	-0.217	0.033
11	-155.20045	19.29218	0.418	-0.468	-0.241	0.040	0.040	0.020
12	-155.19545	19.29633	1.657	-2.254	-1.705	0.230	0.230	0.048
13	-155.18964	19.29919	0.000	0.000	-9.500	0.000	0.000	1.000
14	-155.18570	19.30122	1.537	-3.310	-3.255	0.151	0.151	0.151
15	-155.18425	19.30272	0.923	-1.270	-4.269	0.010	0.010	0.150
16	-155.18188	19.30319	0.000	0.000	-5.563	0.000	0.000	0.150
17	-155.17612	19.30558	0.000	0.000	-3.785	0.000	0.000	0.150
18	-155.18411	19.31604	-0.398	-3.594	-6.269	0.102	0.102	0.102
19	-155.18071	19.31654	-1.794	-9.783	-8.097	0.036	0.036	0.036
20	-155.17717	19.31527	0.206	-1.272	-1.843	0.020	0.020	0.151
21	-155.13411	19.31353	2.061	-5.807	-2.192	0.151	0.151	0.151
22	-155.13411	19.31353	0.337	-2.260	-0.520	0.151	0.151	0.151
23	-155.13330	19.31360	0.000	0.000	0.000	0.000	0.000	0.000
24	-155.13174	19.31386	0.007	0.039	0.000	0.020	0.020	0.020
25	-155.13127	19.30967	0.651	-2.612	0.000	0.050	0.050	0.050
26	-155.13086	19.31022	-0.111	-2.720	0.004	0.212	0.212	0.212
27	-155.12730	19.31056	0.312	-1.695	-0.634	0.062	0.062	0.062
28	-155.14566	19.31005	0.934	-2.486	-1.244	0.220	0.220	0.047
29	-155.14153	19.30617	0.044	-0.037	-0.028	0.026	0.026	0.026
30	-155.11888	19.31188	-0.282	-1.053	0.000	0.000	0.000	0.000
31	-155.12286	19.31149	-0.150	-2.148	-1.097	0.000	0.000	0.100
32	-155.12701	19.31022	0.086	-0.490	-0.191	0.000	0.000	0.100
33	-155.17058	19.31576	0.211	-1.206	-0.060	0.048	0.048	0.096
34	-155.16826	19.31571	-0.004	-1.389	0.079	0.046	0.046	0.092
35	-155.16675	19.31574	-0.018	-1.482	-0.225	0.040	0.040	0.080
36	-155.16566	19.31563	-0.066	-1.469	-0.293	0.046	0.046	0.092
37	-155.16417	19.31602	-0.265	-1.936	-0.183	0.053	0.053	0.106
38	-155.16325	19.31552	-0.136	-2.424	-0.978	0.022	0.022	0.022
39	-155.16324	19.31552	0.199	-1.614	-1.515	0.026	0.026	0.103
40	-155.16861	19.31053	0.125	-0.884	-0.249	0.037	0.037	0.075
41	-155.16701	19.31091	0.114	-0.931	-0.143	0.022	0.022	0.045
42	-155.16579	19.31109	0.101	-0.970	-0.303	0.024	0.024	0.049
43	-155.16393	19.31120	0.132	-0.913	-0.632	0.024	0.024	0.049
44	-155.16333	19.31109	0.325	-0.974	-0.351	0.026	0.026	0.053
45	-155.16312	19.31104	-0.001	-0.004	-2.130	0.010	0.010	0.010
46	-155.16293	19.31104	0.000	-0.002	-1.400	0.010	0.010	0.010
47	-155.15874	19.31617	-0.159	-2.448	-0.792	0.045	0.045	0.045
48	-155.15331	19.31437	-0.823	-1.466	-0.860	0.044	0.044	0.044
49	-155.16620	19.28524	-0.021	-0.067	0.010	0.010	0.010	0.020
50	-155.16357	19.28614	0.284	-0.313	0.030	0.014	0.014	0.028
51	-155.15904	19.28589	0.048	-0.043	0.080	0.010	0.010	0.020
52	-155.15553	19.28612	0.169	-0.220	-0.020	0.010	0.010	0.020
53	-155.17479	19.30776	0.105	-0.350	-0.239	0.035	0.035	0.035
54	-155.14995	19.28950	0.246	-0.349	-0.110	0.014	0.014	0.028
55	-155.14859	19.29066	0.118	-0.497	0.030	0.026	0.026	0.053
56	-155.14777	19.29099	0.330	-0.750	-0.432	0.020	0.020	0.040
57	-155.14690	19.29120	0.193	-0.203	-0.040	0.010	0.010	0.020
58	-155.13585	19.29210	0.102	-0.210	-0.070	0.014	0.014	0.028
59	-155.13324	19.29446	0.150	-0.241	-0.030	0.010	0.010	0.020
60	-155.13107	19.29520	0.046	-0.170	-0.120	0.010	0.010	0.020
61	-155.14407	19.31076	-0.053	-1.152	-0.532	0.044	0.044	0.044

Table 1. (continued)

Traverse	Longitude	Latitude	Offset, m			Error Bound, m		
			East	North	Vertical	East	North	Vertical
62	-155.15124	19.31264	-0.988	-1.160	-1.160	0.044	0.044	0.044
63	-155.21916	19.31570	0.000	0.000	-9.100	0.000	0.000	1.000
64	-155.21942	19.31559	0.000	0.000	-7.000	0.000	0.000	1.000
65	-155.22199	19.31468	0.000	0.000	-4.000	0.000	0.000	1.000
66	-155.20717	19.32176	-0.054	-0.425	-0.058	0.020	0.020	0.020
67	-155.15141	19.28859	0.082	-0.626	-0.020	0.010	0.010	0.020
68	-155.17299	19.31604	0.000	-1.724	-1.054	0.040	0.040	0.040
69	-155.24994	19.28922	0.154	-0.724	-1.452	0.010	0.010	0.010
70	-155.25243	19.31877	0.246	-1.073	-4.990	0.017	0.017	1.000
71	-155.23676	19.31898	0.000	0.000	-2.000	0.000	0.000	1.000
72	-155.24316	19.30313	0.000	0.000	-4.200	0.000	0.000	1.118
73	-155.24538	19.31255	0.133	-1.763	-5.353	0.142	0.142	1.118
74	-155.20662	19.28799	0.635	-0.766	-1.348	0.173	0.173	0.332
75	-155.21561	19.28135	1.007	-2.209	-2.586	0.046	0.046	0.046
76	-155.21884	19.31234	0.448	-0.297	-0.055	0.017	0.017	0.017
77	-155.22593	19.31507	0.000	0.000	-5.800	0.000	0.000	1.414
78	-155.16358	19.31458	-0.563	-2.158	-0.914	0.147	0.147	0.147
79	-155.16251	19.31564	0.002	-2.710	-4.850	0.544	0.544	0.772
80	-155.23152	19.27746	-1.413	-1.096	-1.385	1.025	1.020	1.030
81	-155.24019	19.26976	1.658	-0.438	-9.557	0.246	0.246	1.030
82	-155.22875	19.27714	-2.244	-4.127	-0.984	0.540	0.540	0.540
83	-155.17664	19.31519	-0.119	-1.351	-2.576	0.116	0.116	1.007
84	-155.17591	19.30748	1.468	-1.523	-0.716	0.057	0.057	0.501
85	-155.22442	19.30193	0.054	-1.415	-3.687	0.243	0.243	0.845

[a]See text for method for calculating error bounds of offset. Longitude and latitude for fault offset indicate location of north end of fault traverse.

First, a prehistoric lava flow crossed the Hilina faults sometime in the past. Second, numerous prehistoric earthquakes produced fault offset across the prehistoric lava flow. Third, a Mauna Ulu lava flow then partially filled in the prehistoric fracture sometime between 1969 and 1974. Fourth and most recently, the Kalapana earthquake in 1975 again widened the fracture in the prehistoric lava flow and also created a new fracture in the Mauna Ulu lava flow. We compare the total fault offset in the prehistoric lava flow with fault offset from the Kalapana earthquake in the Mauna Ulu lava flow to estimate the recurrence of large earthquakes. Double-fracture outcrops are identified at three locations in the Hilina fault system (lettered locations in Figure 4). Total fault offsets in the Mauna Ulu lava flows vary from 5 to 67 cm, while total fault offsets in prehistoric lava flows vary from 80 to 89 cm (Table 3).

We evaluate the time-averaged fault offset rate for the Hilina faults using three methods: (1) fault offset rate for each individual traverse; (2) average fault offset rate on a single fault; and (3) total fault offset rate across the Hilina fault system. Time-averaged fault offset rates for individual traverses in prehistoric lava flows are presented in Figure 7. Fault offset data from prehistoric lava flows divided by the age of the lava flow equal the fault offset rate for each traverse. Solid vectors indicate locations with both horizontal and vertical fault offset measurements, whereas open vectors and white dots indicate traverses lacking horizontal or vertical fault offset measurements. Figure 7 simplifies the south flank faults and lava flow geometry and preserves spatial relationships between lava flows and faults. Considering the fault offsets in lava flows for ages back to 1500-3000 years B.P., the maximum horizontal and vertical fault offset rates are approximately 10 and -20 mm/yr, respectively. A negative vertical fault offset rate indicates that the hanging wall moved down relative to the footwall.

Average fault offset rates calculated for the Poliokeawe Pali, Holei Pali, and Apua Pali faults are presented in Figure 8. The Poliokeawe Pali and Holei Pali faults have greater horizontal and vertical fault offsets than compared to the Apua Pali fault. The maximum average horizontal fault offset rate for traverses located in lava flows <750 years B.P. age is 4.6 mm/yr for the Holei Pali fault, while the Poliokeawe Pali fault yields a maximum vertical fault offset rate of -5.6 mm/yr (open symbols in Figures 8a and 8b). A negative vertical fault offset rate indicates downward motion of the hanging wall relative to the footwall. Horizontal and vertical fault offset rates on the Holei Pali fault based on a lava flow of age 750-1500 years B.P. (solid symbol in Figures 8a and 8b) fall between the range of values calculated for fault offset rates in younger lava flows.

To evaluate fault offset and fault offset rates across the entire Hilina fault system, we select multiple traverses that descend across the Hilina fault system on a lava flow of the same age (Figure 9a). Eight traverses (1-8) extend generally north-south across the Hilina fault system. Traverse 1 occurs in a lava flow of age 2350-2450 years B.P., traverses 2 and 3 in lava flows of 1500-3000 years B.P. age and 750-1500 years B.P. age, respectively, and traverses 4-8 in lava flows of 200-750 years B.P. age. For south flank lava flows of <750 years B.P. age, the maximum horizontal fault offset is 7±2 m and

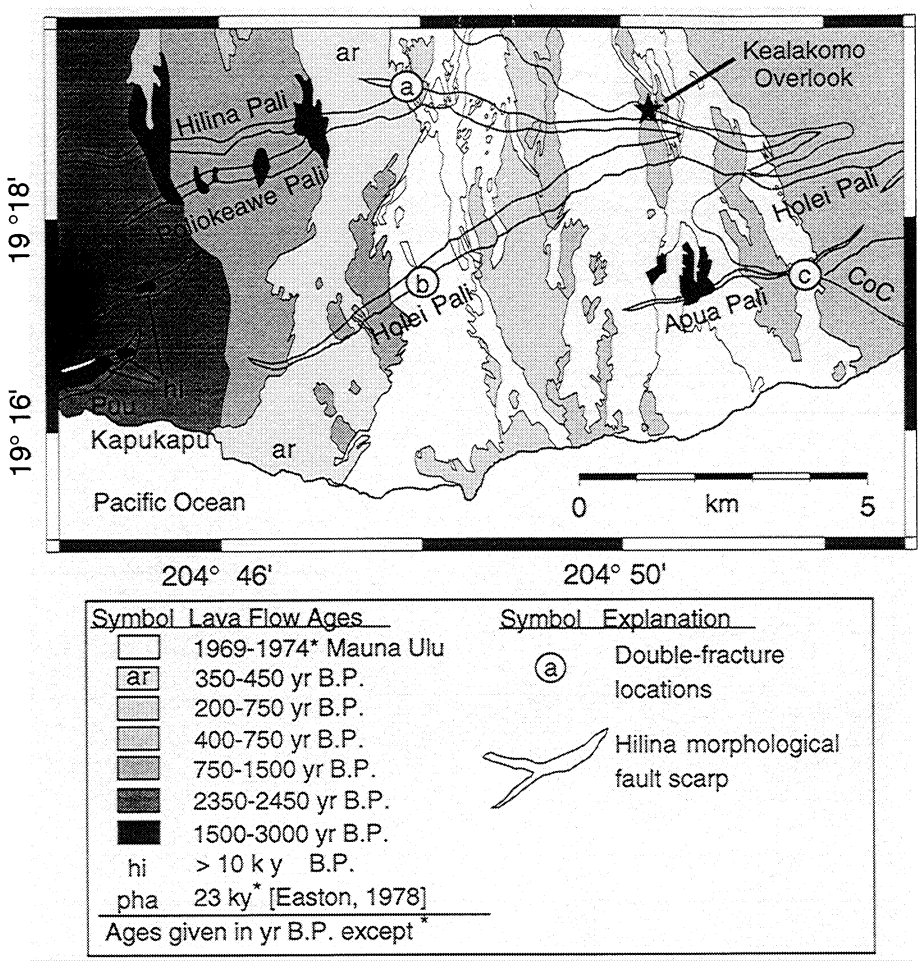

Figure 4. Geologic map of south flank of Kilauea Volcano, Hawaii. Map modified from *Wolfe and Morris* [1996]. Lettered locations a-c identify double-fracture outcrop locations (Table 3). Chain of Craters Road labeled (CoC).

the maximum vertical fault offset is 10±1 m (Figures 9b and 9c). For lava flows <750 years B.P. age, horizontal and vertical fault offset rates across the Hilina fault system range from 4.0 to 12.0 mm/yr and -2.0 to -20.0 mm/yr, respectively (Figures 9b and 9c). Horizontal fault offset rates for lava flows >750 years B.P. age fall below the minimum value of 4.0 mm/yr based on lava flow ages of <750 years B.P. age. Vertical fault offset rates in lava flows >750 years B.P. age exist within the range of fault offset values for lava flow <750 years B.P. age.

7. Discussion

We evaluate the past faulting behavior of the Hilina fault system by discussing our observations and analysis of fractures and fault offsets contained in the prehistoric and Mauna Ulu lava flows. First, we address the limitations of our interpretations imposed by the large uncertainties of lava flow ages and our inability to assign ages to individual prehistoric earthquakes. We then characterize the past faulting behavior of the Hilina faults by (1) interpreting ground fractures from the Kalapana earthquake; (2) comparing fault offsets associated with the Kalapana and prehistoric earthquakes; (3) discussing the plunge of slip vectors for individual traverses, individual Hilina faults, and across the Hilina fault system to support a model of hanging wall rotation; (4) establishing an initial estimate of the number of large (M>7) earthquakes to have occurred in the last ~3000 years; and (5) discussing our assumption 4 of a characteristic large (M>7) earthquake similar to the Kalapana earthquake.

The wide range in lava flow ages results from the scarcity of lava flows dated with radiocarbon or paleomagnetic secular variation methods. At the present, *Wolfe and Morris* [1996] offer the most thorough compilation of ages for lava flows that cover the Hilina fault system (an area 30 km long with 7 km maximum width). As more accurate ages of lava flows become available in the future, the reliability of values for fault offset rate calculations will improve. Our field observations of prehistoric lava flows and fault offsets only provide a maximum age of fault offset based on the age of the lava flow. No minimum age, that is, the age of each earthquake, can be determined from our field observations of fault offset. Perhaps surface dating techniques (i.e., cosmogenic radionuclide) might yield the exposure age of a fault surface to the atmosphere and improve the minimum age estimate for fault offset. Our conclusions are an important first step in determining the past faulting behavior of the Hilina fault system and will benefit from future age determinations of lava flows.

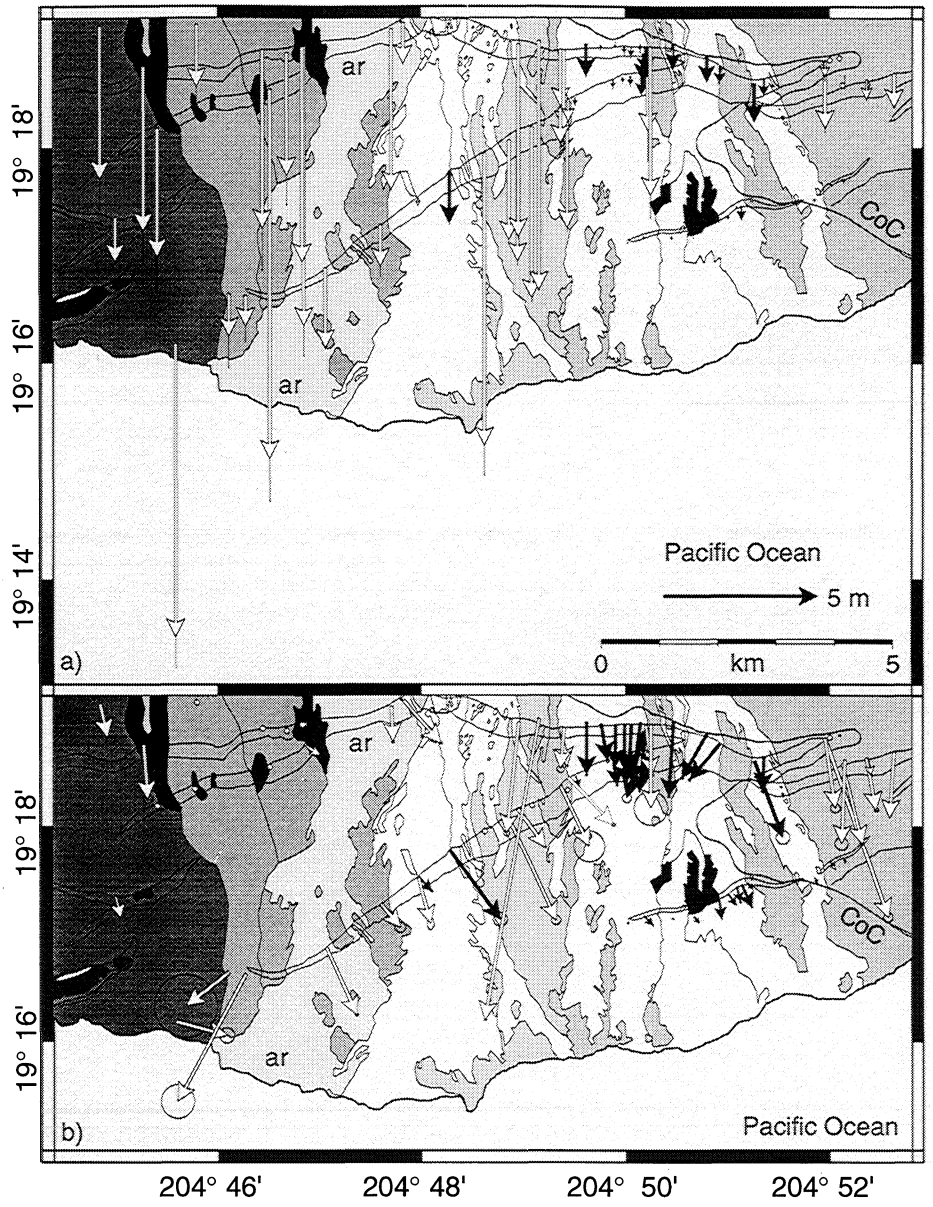

Figure 5. Maps of (a) vertical fault offsets and (b) horizontal fault offsets along Hilina fault system. Solid vectors indicate fault offsets in 1969-1974 Mauna Ulu lava flows, open vectors indicate fault offsets in prehistoric lava flows (ages defined in Figure 4), and scale vector is 5 m with measurement error bounds shown; Chain of Crater Road labeled (CoC). South trending vectors in Figure 5b indicate hanging wall-down fault offset.

We interpret the formation of fractures in Mauna Ulu lava flows associated with the Kalapana earthquake as tectonic in origin. Compressional fold and fault structures are not observed at the base of fault scarps, indicating surficial slumping did not produce the fractures. Where fractures are wide enough to climb down, we examine the fracture walls for piercing points and subsurface detachment surfaces parallel to the base of the lava flows. No subsurface detachment surfaces are observed on fracture walls suggesting the upper few meters of lava flow did not simply detach from the subsurface to produce fractures observed at the surface.

The Kalapana earthquake and prehistoric fault offsets display similar slip vectors. Comparing azimuths of slip vectors, horizontal offsets in the Mauna Ulu lava flows (solid vectors in Figure 5) show motion toward the south in agreement with the overall southeast direction of south flank

Table 2. Average Plunge of Slip Vectors From Fault Traverses Across Hilina Fault System[a]

Earthquake(s)	Poliokeawe Pali	Holei Pali	Apua Pali	All Faults
Kalapana	23°±24°; n=12	23°±07°; n=15	13°±15°; n=9	20°±17°; n=36
Prehistoric	44°±27°; n=8	26°±18°; n=12	20°±14°; n=2	31°±23°; n=22

[a]Average slip vectors format $\mu \pm 1\text{–}\sigma$; n; (μ) mean angular direction; (σ) mean angular deviation; and (n) number of measurements from Figure 5.

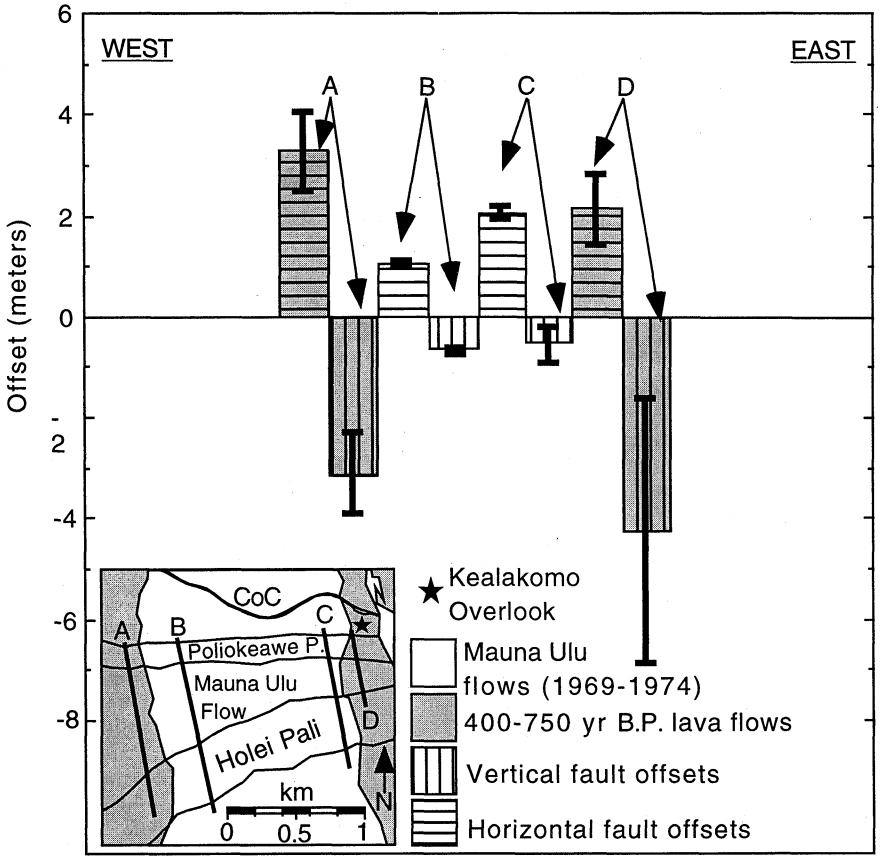

Figure 6. Location map and graph of fault offsets at Kealakomo Overlook site. Chain of Craters Road labeled (CoC).

transport for the Kalapana earthquake [*Tilling et al.*, 1976; *Lipman et al.*, 1985]. The local trend of the Hilina fault traces seems to constrain the fault offsets to trend in a fault-perpendicular direction (*Cannon et al.*, submitted manuscript, 2000]. Considering the plunges of slip vectors, the average plunge of slip vectors for the Hilina faults from the Kalapana earthquake is 20°±17° whereas prehistoric lava flows show 31°±23°. Plunges of slip vectors for the Kalapana earthquake offsets and prehistoric fault offsets suggest that the fault surfaces of the Hilina fault system have an overall dip of less than 45°. The shallow plunge of slip vectors supports our interpretation that the Hilina fault system consists of a series of shallow normal slide blocks rather than deep normal faults (*Cannon et al.*, submitted manuscript, 2000).

These shallow normal slide blocks could accommodate rotation of the hanging wall blocks. If incremental rotation has occurred in the past, the older lava flows faulted by numerous prehistoric earthquakes should have fault offsets with greater vertical components of fault offset compared to horizontal values. For traverses across the Hilina fault system on lava flows older than 750 years B.P. age, the vertical fault offsets are greater than horizontal fault offsets (Figure 9) suggesting incremental rotation has occurred. For lava flows younger than 750 years B.P., individual fault offset traverses (Figures 7 and 8) and traverses across the Hilina fault system (Figure 9) show similar values for horizontal and vertical fault offsets. For the youngest lava flows (1969-1974 Mauna Ulu lava flows) the Kalapana earthquake shows predominantly horizontal fault offsets (Figure 5). Thus the older lava flows have probably experienced more hanging wall rotation than the younger lava flows.

We estimate the number of large earthquakes and their time-averaged recurrence intervals for the Poliokeawe Pali and Holei Pali faults at the Kealakomo Overlook (Figure 6). Comparing fault offset traverses A and B, three to five Kalapana earthquakes could have produced fault offsets observed in the 400-750 years B.P. age lava flows. The time-averaged recurrence intervals for Kalapana earthquakes from traverses A and B are 260-80 years. Horizontal fault offsets are about equal for fault offset traverses C and D. However, the vertical fault offset in traverse D may be explained by as many as seven Kalapana fault offsets. The large error bars on traverse D result from poor scarp preservation.

Interpreting fault offsets at double-fracture outcrops also provides estimates for the number of past large earthquakes and recurrence intervals (Table 3). Assuming that multiple Kalapana earthquakes produced the total fault offset observed in the prehistoric lava flow, 1.2-17.5 Kalapana earthquakes with time-averaged recurrence intervals of 650 to 20 years may have occurred on the Hilina faults. Since fault offsets at double-fracture outcrops may be greatly influenced by local faulting characteristics, the time-averaged recurrence intervals calculated from fault traverses spanning multiple fractures and multiple faults (i.e., Kealakomo Overlook) provide more confident values for recurrence interval estimates.

Our recurrence interval estimates for large south flank earthquakes based on fault offsets near the Kealakomo Overlook agree with values determined in previous studies.

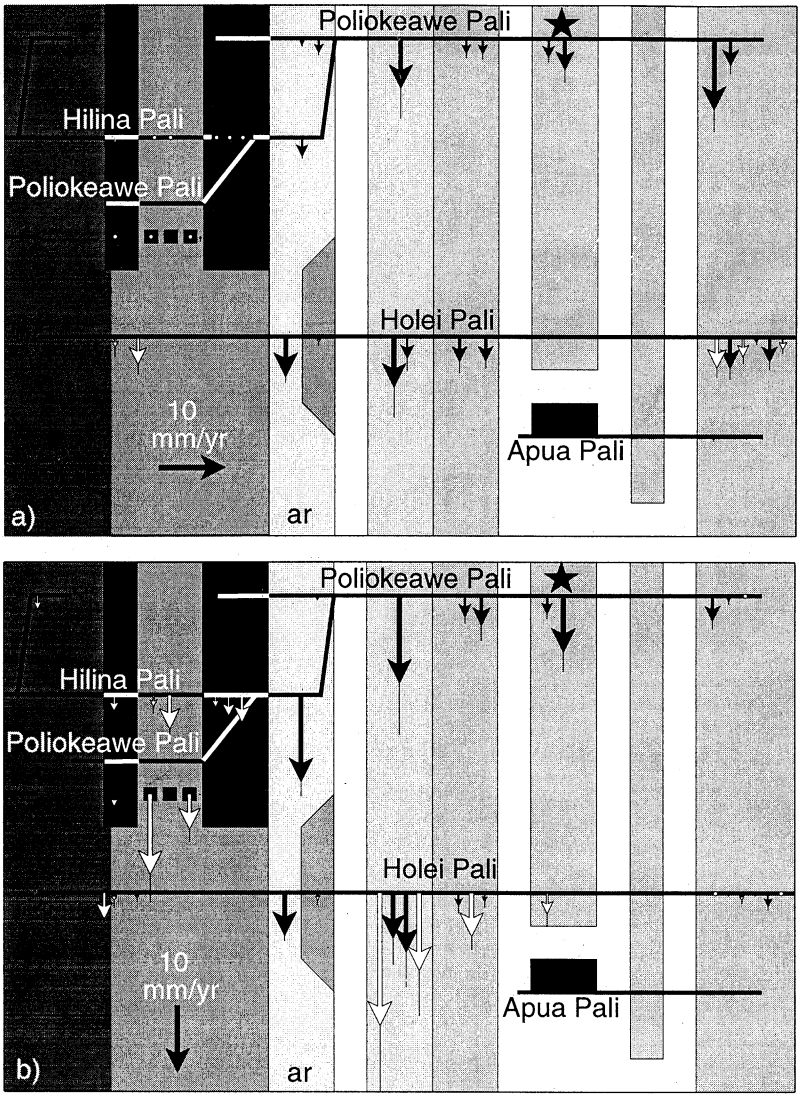

Figure 7. Diagram of (a) horizontal and (b) vertical fault offset rates from historic and prehistoric lava flows. Lava flow ages are from Figure 4; error bounds indicate error propagated from fault offset traverses and lava flow ages. Although not to scale, diagrams preserve spatial relationships between lava flows and faults. Solid vectors indicate locations with both horizontal and vertical fault offset measurements; open vectors and white dots identify locations without both measurements; star indicates location of Kealakomo Overlook. South trending vectors in Figure 7b indicate hanging wall-down fault offset relative to footwall.

The recurrence interval for a $7<M<8$ earthquake in the Kalapana area is 108 years based on the 1868 Great Kau and 1975 Kalapana earthquakes [*Wyss and Koyanagi*, 1992]. *Lipman et al.* [1985] concluded ~1000 Kalapana earthquake subsidence events may be responsible for the Hilina fault scarp morphology. The 23 kyr age of the Pahala ash [*Easton*, 1978] that caps Puu Kapukapu provides a maximum age constraint on the Hilina faults. The recurrence interval for 1000 Kalapana earthquakes over 23 kyr is 230 years. *Riley et al.* [1999] determined a recurrence interval of 200 years from paleomagnetic landward rotations of the block bounded by the Puu Kapukapu and the Hilina faults.

Our estimates for the number of past large south flank earthquake and recurrence intervals depend on the main assumption that all past large earthquakes produced fault offsets comparable to fault offsets measured in the Hilina fault system for the Kalapana earthquake. We are forced into this assumption for two reasons: (1) the Kalapana earthquake is the only earthquake in the twentieth century to produce rupture of the Hilina fault system, and (2) no crosscutting relationships in the field were observed between faults and lava flows to identify individual fault slip associated with individual seismic events. Figure 3 represents the first detailed map of surface rupture created for the Kalapana earthquake. Our wide ranges of estimates for recurrence intervals and the number of large earthquakes suggest that slip on Hilina fault systems is probably not uniform and periodic for past earthquakes. The variations are also due in part to large uncertainties in the ages of lava flows. It is conceivable at the Kealakomo Overlook that fault offsets observed in the Poliokeawe Pali and Holei faults were produced by only two earthquakes since 400-750 years B.P., the 1975 Kalapana and

Table 3. Summary of South Flank Double-Fracture Locations

Location[a]	Mauna Ulu Flow	Older Flow			
	1975 Offset,[b] cm	Total Offset, cm	^{14}C age,[c] years B.P.	Number of Kalapana Events[d]	Recurrence Interval,[e] years
A, Poliokeawe Pali	29	90	350-450	3.1	120-150
B, Holei Pali	67	80	200-750	1.2	190-650
C, Apua Pali	5	89	400-750	17.5	20-40

[a]See Figure 4 for location.

[b]Total offset assumed from 1975 Kalapana earthquake.

[c]Add 25 years for age relative to 1975 Kalapana earthquake.

[d]Number of Kalapana events is total offset from prehistoric lava flow divided by total offset from Mauna Ulu Lava flow.

[e]Recurrence interval (upper limit) is upper value for ^{14}C age relative to Kalapana earthquake divided by number of Kalapana-sized events, and recurrence interval (lower limit) is lower value of ^{14}C age relative to Kalapana earthquake divided by number of Kalapana-sized events.

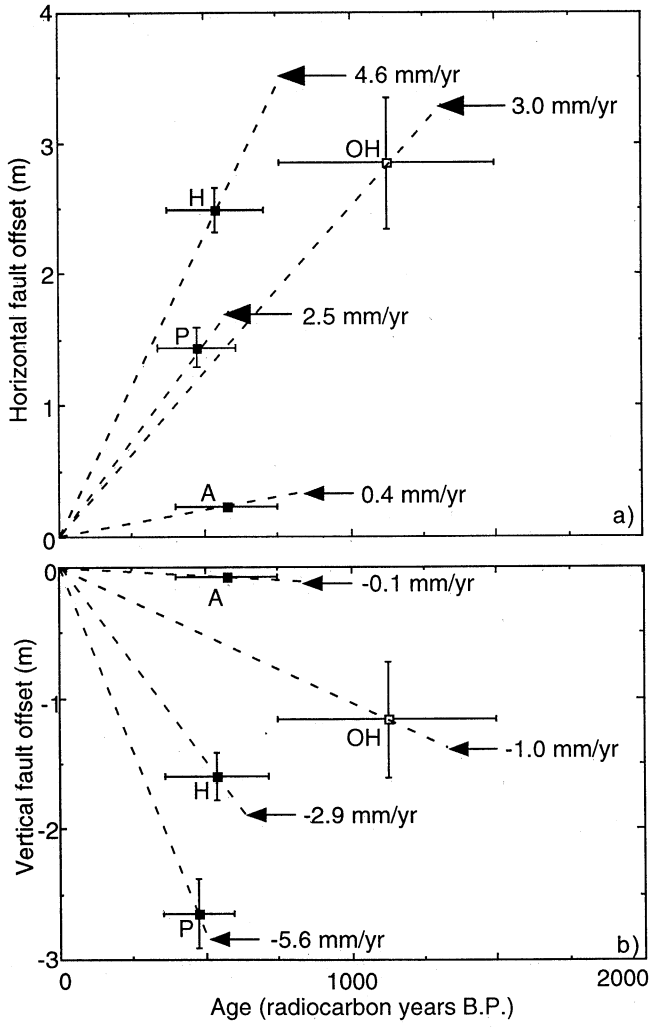

Figure 8. Graphs of average (a) horizontal and (b) vertical fault offsets (from Figures 5b and 5a) verses lava flow age (from Figure 4) for individual fault offset traverses along Hilina fault system. Solid symbols indicate lava flow ages <750 years B.P.; open symbol is for lava flow of 750-1500 years B.P. age. Abbreviations represent A, Apua Pali; H, Holei Pali; P, Poliokeawe Pali; and OH, Holei Pali. Horizontal error bars indicate range of lava flow age estimate; vertical error bars are standard deviation of average fault offsets. Slope of dashed line represent fault offset rates. Negative slope indicates hanging wall-down fault offset relative to footwall.

1868 Great Kau earthquakes. We speculate that the larger magnitude Great Kau earthquake may have produced more slip on the Hilina fault system than occurred with the Kalapana earthquake.

Caution must be exercised with these recurrence interval estimates of large earthquakes in a volcanic system. Volcanic processes and changes through time, such as changes in magma transport, may play an important role in developing and triggering a large earthquake and producing nonuniform recurrence intervals. Whereas plate boundary earthquakes are due to steady loading at the plate boundaries, volcanic systems have loading events that vary drastically on all timescales. The 1975 Kalapana and 1868 Great Kau earthquakes were two very different events, which brings into question the assumption we and other researchers have made about a Kalapana-type "characteristic" earthquake.

8. Conclusions

We document and characterize the faulting behavior of the Hilina fault system by (1) producing the first detailed map of surface rupture for the 1975 Kalapana earthquake and (2) analyzing fault offsets of historic and prehistoric lava flows. Accounts of historical earthquakes on the Island of Hawaii begin in 1823, but we extend the earthquake record as far back as 1500-3000 years B.P. by comparing fault offsets in prehistoric lava flows with neighboring fault offsets from the Kalapana earthquake. We draw several conclusions about the past faulting behavior of the Hilina fault system from our analysis:

1. For the time period back to 750 years B.P., horizontal and vertical fault offset rates for individual Hilina faults reach a maximum of 4.6 and -5.6 mm/yr, respectively. Also, horizontal and vertical fault offset rates across the entire Hilina fault system are 4.0 to 12.0 and -2.0 to -20.0 mm/yr, respectively. Negative vertical fault offset rates indicate hanging wall down motion relative to the footwall.

2. Average plunges of slip vectors for the Kalapana earthquake and fault offsets in prehistoric lava flows are 20°±17° and 31°±23°, respectively. The Hilina faults are probably shallow normal faults rather than steep and deep-rooted normal faults. The older lava flows faulted by numerous prehistoric earthquakes show fault offsets with greater vertical fault offsets than horizontal fault offsets, suggesting that rotation of hanging wall blocks has occurred within the Hilina fault system.

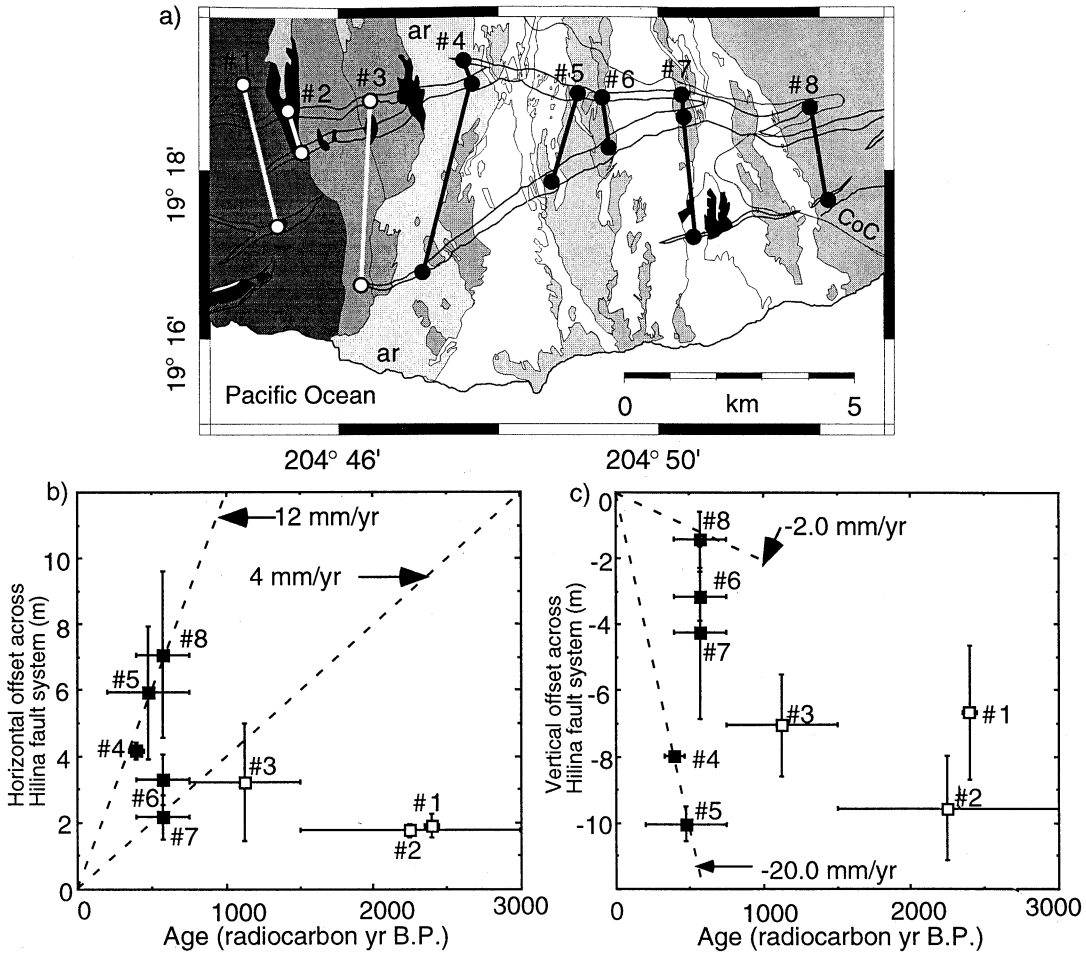

Figure 9. (a) Map of traverse locations (dots; data from Figure 5) used to construct fault offset traverses across the Hilina fault system. White dots connected with white lines represent traverses on lava flows older than 750 years B.P., solid dots connected with black lines indicate traverses on lava flows younger than 750 years B.P. Lava flows for traverses are 1, 2350-2450 years B.P.; 2, 1500-3000 years B.P.; 3, 750-1500 years B.P.; 4, 330-470 years B.P.; 5, 200-750 years B.P.; 6-8, 400-750 years B.P (lava flow ages from Figure 4). (b) and (c) Horizontal and vertical fault offset across Hilina fault system. Slope of dashed lines represent envelope of possible fault offset rates. Numbered symbols correspond to traverse numbers in Figure 9a. Horizontal error bars indicate age range of lava flow age estimate, and vertical error bars indicate measurement error of fault offset and range of summed offset values. Negative slope indicate hanging wall-down fault offset relative to footwall.

3. Assuming that each prehistoric faulting event produced fault offsets along the Hilina fault system similar to fault offsets measured for the Kalapana earthquake, three to five Kalapana events probably occurred since 400-750 years B.P. with recurrence intervals of 260-80 years. However, the wide range in estimates for the number of prehistoric faulting events, in part due to large uncertainties in lava flow ages, suggests that these prehistoric events may not have produced fault offsets similar to the Kalapana earthquake. These prehistoric events probably did not have uniform recurrence intervals either.

4. Some or all of the prehistoric fault offsets of age less than 750 years B.P. on the Poliokeawe Pali and Holei Pali faults at the Kealakomo Overlook may be explained by just two earthquakes, the 1975 Kalapana and 1868 Great Kau earthquakes.

Our work supplies crucial fault offset information to improve earthquake hazard assessment of the south flank. However, our efforts are limited by the extent of the Mauna Ulu lava flows and prehistoric lava flows that have preserved piercing points and by the scarcity of accurate lava flow ages. At this time, geodetic monitoring of strain accumulation across the south flank and seismic monitoring are better suited to directly evaluate future earthquake hazards on the south flank.

Acknowledgments. This work was supported by a U.S. Geological Survey National Earthquake Hazards Reduction Program grant 14534-HQ-98-GR-1024, a Geological Society of America Student Research grant (E.C.C.), and a University of California, Davis Cordell Durrell grant (E.C.C.). Robert Twiss, James McClain, Richard Fiske, Alan Linde, and Will Prescott provided comments that significantly improved this manuscript. We received help from many people at the Hawaiian Volcano Observatory, especially Don Swanson, Michael Lisowski, Asta Miklius, Kristine Larson, Taeko Jane Takahashi, Arnold Okamura, and Paul Okubo. We thank James Kellogg and William Chadwick for providing fault offset data and field notes from their Hilina fieldwork. We appreciate the excellent efforts of our field assistants Jason Bariel, Chad Fleschner, Mike Poland, Gwen Pikkarainen, and Jim Weigel. Many figures were

produced with Generic Mapping Tool software [*Wessel and Smith*, 1995]. Additional information available at:
http://perry.geo.berkeley.edu/~burgmann/RESEARCH/research.html

References

Ando, M., The Hawaii earthquake of November 29, 1975: Low dip angle faulting due to forceful injection of magma, *J. Geophys. Res., 94*, 7616-7626, 1979.

Brigham, W. T., The volcanoes of Kilauea and Mauna Loa on the island of Hawaii, *Mem. Bernice Pauahi Bishop Mus., 2*, 478-497, 1909.

Chadwick Jr., W. W., J. R. Smith Jr., J. G. Moore, D. A. Clague, M. O. Garcia, and C. G. Fox, Bathymetry of south flank of Kilauea Volcano, *U.S. Geol. Surv. Misc. Field Stud. Map, MF-2231*, 1993.

Delaney, P. T., R. Denlinger, M. Lisowski, A. Miklius, P. Okubo, A. Okamura, and M. K. Sako, Volcanic spreading at Kilauea, 1976-1996, *J. Geophys. Res., 103*, 18,003-18,023, 1998.

Denlinger, R. P., and P. Okubo, Structure of the mobile south flank of Kilauea, Volcano, Hawaii, *J. Geophys. Res., 100*, 24,499-24,507, 1995.

Dieterich, J. H., Growth and persistence of Hawaiian volcanic rift zones, *J. Geophys. Res., 93*, 4258-4270, 1988.

Easton, R. M., The stratigraphy and petrology of the Hilina Formation: The oldest exposed lavas of Kilauea Volcano, Hawaii, M.S. thesis, Univ. of Hawaii, Honolulu, 1978.

Fiske, R. S., and E. D. Jackson, 1972, Orientation and growth of Hawaiian volcanic rifts: The effect of regional structure and gravitational stresses, *Proc. R. Soc. London, 329*, 299-326, 1972.

Flanigan, V. J., and C. L. Long, Aeromagnetic and near-surface electrical expression of the Kilauea and Mauna Loa volcanic rift systems, *U.S. Geol. Surv. Prof. Pap., 1350*, 935-946, 1987.

Furumoto, A. S., and R. L. Kovach, The Kalapana earthquake of November 28, 1975: An intra-plate earthquake and its relation to geothermal processes, *Phys. Ear. Plan. Inter., 18*, 197-208, 1979.

Gillard, D., M. Wyss, and P. Okubo, Type of faulting and orientation of stress and strain as a function of space and time in Kilauea's south flank, Hawaii, *J. Geophys. Res., 101*, 16,025-16,042, 1996.

Got, J.-L., F. W. Fréchet, and W. Klein, Deep fault plane geometry inferred from multiplet relative relocation beneath the south flank of Kilauea, *J. Geophys. Res., 99*, 15,375-15,386, 1994.

Hill, D. P., Crustal structure of the island of Hawaii from seismic-refraction measurements, *Bull. Seismol. Soc. Am., 59*, 101-130, 1969.

Hill, D. P., and J. J. Zucca, Geophysical constraints on the structure of Kilauea and Mauna Loa Volcanoes and some implications for seismomagnetic processes, *U.S. Geol. Surv. Prof. Pap., 1350*, 903-917, 1987.

Holcomb, R. T., Eruptive history and long-term behavior of Kilauea Volcano, *U.S. Geol. Surv. Prof. Pap., 1350*, 261-350, 1987.

Lipman, P. W., J. P. Lockwood, R. T. Okamura, D. A. Swanson, and K. M. Yamashita, Ground deformation associated with the 1975 magnitude-7.2 earthquake and resulting changes in activity of Kilauea Volcano, Hawaii, *U.S. Geol. Surv. Prof. Pap., 1276*, 1985.

Lockwood, J. P., and P. W. Lipman, Recovery of datable charcoal beneath young lavas: Lessons from Hawaii, *Bull. Volcanol., 43*, 609-615, 1980.

Ma, K.-F., H. Kanamori, and K. Satake, Mechanism of the 1975 Kalapana, Hawaii, earthquake inferred from tsunami data, *J. Geophys. Res, 104*, 13,153-13,167, 1999.

Moore, J. G., W. B. Bryan, M. H. Beeson, and W. R. Normark, Giant blocks in the South Kona landslide, Hawaii, *Geology, 23*, 125-128, 1995.

Morgan, J. K., G. F. Moore, D. J. Hill, and S. Leslie, Overthrusting and sediment accretion along Kilauea's mobile south flank, Hawaii: Evidence for volcanic spreading from marine seismic reflection data, *Geology, 28*, 667-670, 2000.

Nakamura, K., Why do long rift zones develop better in Hawaiian volcanoes? A possible role of thick ocean sediment, *Bull. Volcanol. Soc. J., 25*, 255-269, 1980.

Okubo, P. G., H. M. Benz, and B. A. Chouet, Imaging the crustal magma sources beneath Mauna Loa and Kilauea Volcanoes, Hawaii, *Geology, 25*, 867-870, 1997.

Owen, S., P. Segall, J. Freymueller, A. Miklius, R. Denlinger, T. Árnadóttir, M. Sako, and R. Bürgmann, Rapid deformation of the south flank of Kilauea Volcano, Hawaii, *Science, 267*, 1328-1332, 1995.

Owen, S., P. Segall, M. Lisowski, A. Miklius, R. Denlinger, J. Freymueller, T. Árnadóttir, and M. Sako, Rapid deformation of Kilauea Volcano: Global Positioning System measurements between 1990 and 1996, *J. Geophys. Res., 105*, 18,983-18998, 2000.

Riley, C. M., J. F. Diehl, J. L. Kirschvink, and R. L. Ripperdan, Paleomagnetic constraints on fault motion in the Hilina fault system, south flank of Kilauea Volcano, Hawaii, *J. Volcanol. Geotherm. Res., 94*, 233-249, 1999.

Smith, J. R., A. Malahoff, and A. N. Shor, Submarine geology of the Hilina slump and morpho-structural evolution of Kilauea Volcano, Hawaii, *J. Volcanol. Geotherm. Res., 94*, 59-88, 1999.

Swanson, D. A., W. A. Duffield, and R. S. Fiske, Displacement of the south flank of Kilauea Volcano: the result of forceful intrusion of magma into the rift zones, *U.S. Geol. Surv. Prof. Pap., 963*, 1974.

Thurber, C. H. and A. E. Gripp, Flexure and seismicity beneath the south flank of Kilauea volcano and tectonic implications, *J. Geophys, Res., 93*, 4271-4281, 1988.

Tilling, R. I., R. Y. Koyanagi, P. W. Lipman, J. P. Lockwood, J. G. Moore, and D. A. Swanson, Earthquake and related catastrophic events Island of Hawaii, November 29, 1975: A preliminary report, *U. S. Geol. Surv. Circ., 740*, 1976.

Wessel, P., and W. H. F. Smith, New version of the Generic Mapping Tools released, *EOS Trans. AGU, 76*, 329, 1995.

Wolfe, E. W., and J. Morris, Geologic map of the Island of Hawaii, *U.S. Geol. Surv. Misc. Invest. Ser. Map, I-2524-A*, 1996.

Wyss, M., A proposed source model for the Great Kau, Hawaii, earthquake of 1868, *Bull. Seismol. Soc. Am., 78*, 1450-1462, 1988.

Wyss, M., and R. Y. Koyanagi, Seismic gaps in Hawaii, *Bull. Seismol. Soc. Am., 82*, 1373-1387, 1992.

R. Bürgmann, Department of Geology and Geophysics, 307 McCone Hall, University of California, Berkeley, CA 94720-4767. (burgmann@seismo.berkeley.edu)

E. C. Cannon, Department of Geological Sciences, University of Colorado, Boulder, CO 80309-0399. (Eric.Cannon@Colorado.edu)

(Received May 22, 2000; revised October 12, 2000;
accepted November 13, 2000.)